

Calibration of gamma-ray bursts luminosity correlations using gravitational waves as standard sirens

Y. Y. WANG¹ AND F. Y. WANG^{1,2}

¹*School of Astronomy and Space Science, Nanjing University, Nanjing 210093, China*

²*Key Laboratory of Modern Astronomy and Astrophysics (Nanjing University), Ministry of Education, Nanjing 210093, China*

ABSTRACT

Gamma-ray bursts (GRBs) are a potential tool to probe high-redshift universe. However, the circularity problem enforces people to find model-independent methods to study the luminosity correlations of GRBs. Here, we present a new method which uses gravitational waves as standard sirens to calibrate GRB luminosity correlations. For the third-generation ground-based GW detectors (i.e., Einstein Telescope), the redshifts of gravitational wave (GW) events accompanied electromagnetic counterparts can reach out to ~ 4 , which is more distant than type Ia supernovae ($z \lesssim 2$). The Amati relation and Ghirlanda relation are calibrated using mock GW catalogue from Einstein Telescope. We find that the 1σ uncertainty of intercepts and slopes of these correlations can be constrained to less than 0.2% and 8% respectively. Using calibrated correlations, the evolution of dark energy equation of state can be tightly measured, which is important for discriminating dark energy models.

Keywords: gamma-ray burst: general—gravitational waves: standard sirens

1. INTRODUCTION

Gamma-ray burst (GRB) are one of the most energetic phenomena in our Universe (Kumar & Zhang 2015; Wang, Dai & Liang 2015). The high luminosity makes them detectable out to high redshifts. Therefore, GRBs are promising tool to probe the high-redshift universe: including the cosmic expansion and dark energy (Dai, Liang & Xu 2004; Liang & Zhang 2006; Schaefer 2007; Wang, Dai & Zhu 2007), star formation rate (Totani 1997; Bromm, Coppi & Larson 2002; Wang & Dai 2009; Wang 2013), the reionization epoch (Barkana & Loeb 2004; Totani et al. 2006) and the metal enrichment history of the Universe (Wang et al. 2012; Hartoog et al. 2015). Among them, the γ -ray bursts correlations (for reviews, see Wang, Dai & Liang 2015; Dainotti & Del Vecchio 2017; Dainotti, Del Vecchio & Tarnopolski 2018; Dainotti & Amati 2018) are most widely studied, which can not only shed light on the radiation mechanism of GRBs, but also provide a promising tool to probe the cosmic expansion and dark energy (Wang, Dai & Liang 2015; Dainotti & Del Vecchio 2017). These correlations can be divided into three categories, such as prompt correlations, afterglow correlations and prompt-afterglow correlations. The prompt correlations mainly include Amati correlation (Amati et al. 2002), Ghirlanda correlation (Ghirlanda, Ghisellini & Lazzati 2004), Liang-Zhang correlation (Liang & Zhang 2005), Yonetoku correlation (Wei & Gao 2003; Yonetoku et al. 2004) and $L_{\text{iso}} - \tau_{\text{lag}}$ correlation (Norris, Marani & Bonnell 2000). Afterglow correlations contain only parameters in the afterglow phase, such as Dainotti correlation ($L_X(T_a) - T_{X,a}^*$) (Dainotti, Cardone & Capozziello 2008), $L_X(T_a) - T_{X,a}^*$ and $L_O(T_a) - T_{O,a}^*$ correlations (Ghisellini et al. 2009) and $L_{O,200\text{s}} - \alpha_{O,>200\text{s}}$ correlation (Oates et al. 2012). Prompt-afterglow correlations connect plateaus and prompt phases, referring to $E_{\gamma,\text{afterglow}} - E_{X,\text{prompt}}$ correlation (Liang, Zhang & Zhang 2007), $L_{X,\text{afterglow}} - E_{\gamma,\text{prompt}}$ correlation (Berger 2007), $L_X(T_a) - L_{\gamma,\text{iso}}$ correlation (Dainotti 2011), $L_{\text{iso}} - E_{p,z} - \Gamma_0$ correlation (Liang et al. 2015) and so on.

However, there is a circularity problem when treating GRBs as relative standard candles. It arises from the derivation of quantities like luminosity L_{iso} , isotropic energy E_{iso} and collimation-corrected energy E_{γ} , which are dependent on luminosity distance d_L in a fiducial cosmology. For instance, the d_L in a flat Λ CDM model can be expressed as

$$d_L(z) = \frac{c(1+z)}{H_0} \int_0^z \frac{dz'}{\sqrt{\Omega_m(1+z')^3 + (1 - \Omega_m - \Omega_\Lambda)(1+z')^2 + \Omega_\Lambda}}. \quad (1)$$

Therefore, it is inappropriate to use the model-dependent luminosity correlations to study cosmology models in turn. Several approaches have been proposed to overcome the problem (Wang, Dai & Liang 2015; Dainotti & Del Vecchio 2017). One method is to fit the cosmological parameters and luminosity correlation simultaneously (Ghirlanda et al. 2004; Li et al. 2008). Another method is to calibrate the correlations using type Ia supernovae (SNe Ia) (Liang et al. 2008) or observational Hubble Data (OHD) (Amati et al. 2018). It is based on the principle that objects of the same redshift should have same luminosity distance. Wang (2008) pointed out that the GRB luminosity correlations calibrated by SNe Ia are no longer completely independent of the SNe Ia data points. Consequently, the GRB data cannot be combined with the SNe Ia dataset directly to constrain cosmological parameters. What's worse, high redshift SNe Ia can hardly be found and the furthest SN Ia yet seen is GND12Col with $z = 2.26^{+0.02}_{-0.10}$ (Rodney et al. 2015), while the redshift of GRB can be up to 9.4 (Cucchiara et al. 2011). Moreover, there are many some systematic uncertainties for SNe Ia, such as dust in the light path (Avgoustidis, Verdec & Jimenez 2009; Hu, Yu & Wang 2017), the possible intrinsic evolution of SN luminosity, magnification by gravitational lensing (Holz 1998), peculiar velocity (Hui & Greene 2006), and so on. These processes will degrade the usefulness of SNe Ia as standard candles.

Here, we come up with the idea to calibrate GRB luminosity relations using gravitational waves (GW) standard sirens. The detection of GW170817 accompanied by electromagnetic counterparts heralds the new era of gravitational-wave multi-messenger astronomy (Abbott et al. 2017). Schutz (1986) first pointed out that the waveform signals from inspiralling compact binaries can be used to determine the luminosity distance to the source, serving as a standard siren. This kind of standard siren is a self-calibrating distance indicator, which just relying on the modelling of the two-body problem in general relativity (Sathyaprakash, Schutz & Van Den Broeck 2010). The of detected BNS and BH-NS merger events can reach up to $z \sim 4$ to the farthest by Einstein Telescope (ET) (Abernathy et al. 2011; Li 2015; Cai & Yang 2017), going beyond the redshift limitation of SNe Ia. For the third generation detectors, such as ground-based Einstein Telescope (ET) (Abernathy et al. 2011), space-based Big Bang Observer (BBO) (Cutler & Holz 2009), and Deci-Hertz Interferometer Gravitational wave Observatory (DECIGO) (Kawamura et al. 2011), smaller distance uncertainty will be achieved than Advanced LIGO and Virgo (Abbott et al. 2017).

The paper is organized as follows. In Section 2, we introduce the procedure of construction mock GW catalogue. The calibration of GRB luminosity correlations with GW standard sirens is illustrated in Section 3. A summary of our result and future outlooks is provided in the end of the paper.

2. CONSTRUCTION OF GW STANDARD SIRENS

2.1. Redshift distribution

In order to construct a mock GW catalogue, we need to consider the redshift distribution of the sources, which satisfies the following expression

$$P(z) \propto \frac{4\pi d_C^2(z)R(z)}{H(z)(1+z)}, \quad (2)$$

where $d_C(z)$ is the comoving distance of the source. The time evolution of the NS-NS merger rate $R(z)$ is given by (Schneider et al. 2001)

$$R(z) = \begin{cases} 1 + 2z, & z \leq 1 \\ \frac{3}{4}(5 - z), & 1 < z < 5 \\ 0, & z \geq 5. \end{cases} \quad (3)$$

The NS-NS merger rate at redshift z is $\dot{n}(z) = \dot{n}_0 \cdot R(z)$ and the merger rate today is about $\dot{n}_0 = 1.54^{+3.2}_{-1.22} \times 10^{-6} \text{ Mpc}^{-1} \text{ yr}^{-1}$ (Abbott et al. 2017).

2.2. Simulation of luminosity distances

It is necessary to define the total mass $M_{\text{phys}} = m_1 + m_2$, symmetric mass ratio $\eta = \frac{m_1 m_2}{M^2}$ and chirp mass $\mathcal{M}_{c,\text{obs}} = M\eta^{3/5}$ before our analysis, given binary component masses m_1 and m_2 . The observed chirp mass is related to physical chirp mass via $\mathcal{M}_{c,\text{obs}} = (1+z)\mathcal{M}_{c,\text{phys}}$. Similarly, the observed total mass is $M_{\text{obs}} = (1+z)M_{\text{phys}}$.

2.2.1. Frequency domain waveform and Fourier Amplitude

The response of the detector $h(t)$ is a linear combination of two components

$$h(t) = F_+(\theta, \phi, \psi)h_+(t) + F_\times(\theta, \phi, \psi)h_\times(t), \quad (4)$$

where F_+ and F_\times are the antenna pattern functions of the detector, ψ is the polarization angle, and (θ, ϕ) is the location of the source on the sky. The antenna pattern functions of ET are

$$\begin{aligned} F_+^{(1)}(\theta, \phi, \psi) &= \frac{\sqrt{3}}{2} \left[\frac{1}{2} (1 + \cos^2 \theta) \cos 2\phi \cos 2\psi - \cos \theta \sin 2\phi \sin 2\psi \right], \\ F_\times^{(1)}(\theta, \phi, \psi) &= \frac{\sqrt{3}}{2} \left[\frac{1}{2} (1 + \cos^2 \theta) \cos 2\phi \sin 2\psi + \cos \theta \sin 2\phi \cos 2\psi \right]. \end{aligned} \quad (5)$$

The other pattern functions are $F_{+, \times}^{(2)}(\theta, \phi, \psi) = F_{+, \times}^{(1)}(\theta, \phi + 2\pi/3, \psi)$ and $F_{+, \times}^{(3)}(\theta, \phi, \psi) = F_{+, \times}^{(1)}(\theta, \phi + 4\pi/3, \psi)$ respectively. The Fourier transform of time domain waveform $h(t)$ is given by

$$\mathcal{H}(f) = \mathcal{A} f^{-7/6} \exp(i(2\pi f t_0 - \pi/4 + 2\psi(f/2) - \phi_{(2,0)})), \quad (6)$$

where

$$\mathcal{A} = \frac{1}{d_L} \sqrt{F_+^2 (1 + \cos^2 \iota)^2 + 4F_\times^2 \cos^2 \iota} \sqrt{\frac{5\pi}{96}} \pi^{-7/6} \mathcal{M}_{c, \text{obs}}^{5/6}. \quad (7)$$

is the Fourier amplitude. The post-Newtonian formalism of GW waveform phase up to 3.5 PN is used (Blanchet et al. 2002) and the expressions of functions ψ and $\phi_{(2,0)}$ can be found in Arun et al. (2005) and Zhao et al. (2011).

The component masses of binary neutron stars are randomly sampled in $[1, 2] M_\odot$, while for neutron star-black hole systems, the component mass of black hole is uniform in $[3, 10] M_\odot$ (Fryer & Kalogera 2001; Li 2015; Cai & Yang 2017). The beaming angle of γ -ray bursts are randomly sampled in interval $[0^\circ, 20^\circ]$. Since the GW signal-to-noise ratio in Sec. 2.2.2 is independent of the waveform phase, the ψ and $\phi_{(2,0)}$ are not considered here.

2.2.2. The signal-to-noise ratio and estimated error

A GW signal is claimed to be detected only when combined signal-to-noise ratio (SNR) ≥ 8 for a single detector network (Sathyaprakash, Schutz & Van Den Broeck 2010). For ET, The combined SNR is

$$\rho = \sqrt{\sum_{i=1}^3 (\rho^{(i)})^2}, \quad (8)$$

where

$$\rho^{(i)} = \sqrt{\langle \mathcal{H}^{(i)}, \mathcal{H}^{(i)} \rangle}. \quad (9)$$

and the bracket is defined by

$$\langle a, b \rangle = 4 \int_{f_{\min}}^{f_{\max}} \frac{a(f)b^*(f) + a^*(f)b(f)}{2} \frac{df}{S_h(f)}. \quad (10)$$

where $S_h(f)$ is the one-sided noise power spectrum density (PSD), which determines the performance of a GW detector. We take the noise PSD of ET to be

$$S_h(f) = S_0 \left[x^{p_1} + a_1 x^{p_2} + a_2 \frac{1 + b_1 x^1 + b_2 x^2 + b_3 x^3 + b_4 x^4 + b_5 x^5 + b_6 x^6}{1 + c_1 x^1 + c_2 x^2 + c_3 x^3 + c_4 x^4} \right], \quad (11)$$

as in Zhao et al. (2011), where $x \equiv f/200$ Hz and $S_0 = 1.449 \times 10^{52}$ Hz $^{-1}$. The parameters p_i , a_i , b_i and c_i are also provided in Zhao et al. (2011). The upper cutoff frequency f_{\max} is twice the orbit frequency at the last stable orbit, $f_{\max} = 2f_{\text{LSO}} = 2/(6^{3/2} 2\pi M_{\text{obs}})$. The lower cutoff frequency is $f_{\text{lower}} = 1$ Hz.

At every simulated redshift, the fiducial value of the luminosity distance d_L^{fid} is calculated according to Equation 1. Then we simulate the $\ln d_L^{\text{mea}}$ to be Gaussian distribution centered around $\ln d_L^{\text{fid}}$ with standard deviation $\sigma_{\ln d_L}$,

$$\ln d_L^{\text{mea}} = \mathcal{N}(\ln d_L^{\text{fid}}, \sigma_{\ln d_L}). \quad (12)$$

The fiducial cosmology is flat Λ CDM cosmology with $\Omega_m = 0.308$, $H_0 = 67.8$ km s $^{-1}$ Mpc $^{-1}$ (Planck collaboration 2016) when calculating $\ln d_L^{\text{fid}}$.

The Fisher matrix Γ_{ij} is widely used to estimate the errors in the measured parameters,

$$\Gamma_{ij} = \left\langle \frac{\partial \mathcal{H}}{\partial p_i}, \frac{\partial \mathcal{H}}{\partial p_j} \right\rangle. \quad (13)$$

where p_i denotes the parameters on which the waveforms are depending, namely $(\ln \mathcal{M}_c, \ln \eta, t_0, \Phi_0, \cos \iota, \psi, \ln d_L)$. Then the estimated error σ_{p_i} of parameter p_i is $(\Gamma^{-1})_{ii}^{1/2}$. However, for calculation simplicity, we follow [Cai & Yang \(2017\)](#) and take the distance uncertainty $\sigma_{d_L}^{\text{inst}}$ to be $2d_L/\rho$, allowing for the correlation between d_L and ι . When the additional error $\sigma_{d_L}^{\text{lens}}$ due to the weak lensing taken into account, the total uncertainty is

$$\begin{aligned} \epsilon_{d_L} &= \sqrt{(\sigma_{d_L}^{\text{inst}})^2 + (\sigma_{d_L}^{\text{lens}})^2} \\ &= \sqrt{\left(\frac{2d_L}{\rho}\right)^2 + (0.05z d_L)^2} \end{aligned} \quad (14)$$

2.2.3. The predicted event rates

[Abernathy et al. \(2011\)](#) predicted event rates in ET. It is expected to observe $\mathcal{O}(10^3 \sim 10^7)$ BNS merger events and $\mathcal{O}(10^3 \sim 10^7)$ BH-NS events per year. However, this prediction is very uncertain. [Li \(2015\)](#) expected that only a small fraction ($\sim 10^{-3}$) of GW detections are accompanied by observed GRBs. Therefore we typically construct a catalogue of 1000 BNS events in our simulation. Besides, when the ratio between NS-BH and BNS events is assumed to be 0.03 as predicted by Advanced LIGO-Virgo network ([Abadie et al. 2010](#); [Li 2015](#); [Cai & Yang 2017](#)), 30 NS-BH events are included in the mock catalogue. These simulated events can reach out to a redshift $z \sim 4$. [Figure 1](#) shows the d_L - z diagram of our mock GW catalogue.

3. CALIBRATION OF GRB LUMINOSITY CORRELATIONS

The GRB samples used for calibrating Amati relation ($E_{\text{iso}}-E_p$) and Ghirlanda relation ($E_\gamma-E_p$) are taken from [Wang & Wang \(2016\)](#) and [Wang, Qi & Dai \(2011\)](#) respectively.

The energy spectrum of GRBs is modeled by a broken power law ([Band et al. 1993](#))

$$\Phi(E) = \begin{cases} \left(\frac{E}{100 \text{ keV}}\right)^\alpha \exp(-(2+\alpha)E/E_{p,\text{obs}}), & E \leq \frac{\alpha-\beta}{2+\alpha} E_{p,\text{obs}} \\ \left[\frac{(\alpha-\beta)E_{p,\text{obs}}/(2+\alpha)}{100 \text{ keV}}\right]^{\alpha-\beta} \exp(\beta-\alpha)\left(\frac{E}{100 \text{ keV}}\right)^\beta, & \text{otherwise.} \end{cases} \quad (15)$$

where the typical spectral index values are taken to be $\alpha = -1.0$ and $\beta = -2.2$ if they are not given in the references.

For each GRB in the sample, the fluence S have been corrected to 1-10000 keV energy band with k -correction ([Bloom, Frail & Sari 2001](#)),

$$S_{\text{bolo}} = S \times \frac{\int_{1/(1+z)}^{10^4/(1+z)} E\Phi(E)dE}{\int_{E_{\text{min}}}^{E_{\text{max}}} E\Phi(E)dE}, \quad (16)$$

where E_{min} and E_{max} are detection thresholds of the observing instrument. The isotropic energy $E_{\gamma,\text{iso}}$ and collimation-corrected energy E_γ are

$$E_{\gamma,\text{iso}} = \frac{4\pi d_L^2 S_{\text{bolo}}}{1+z}, \quad (17)$$

and

$$E_\gamma = \frac{4\pi d_L^2 S_{\text{bolo}} F_{\text{beam}}}{1+z}. \quad (18)$$

respectively, in which $F_{\text{beam}} = 1 - \cos \theta_{\text{jet}}$ is the beaming factor for jet opening angle θ_{jet} . The luminosity distance d_L of low-redshift GRBs is derived from GW standard sirens using linear interpolation method ([Wang & Wang 2016](#)), which is independent of cosmology models

$$\ln d_L = \ln d_{L,i}^{\text{GW}} + \frac{z - z_i}{z_{i+1} - z_i} (\ln d_{L,i}^{\text{GW}} - \ln d_{L,i+1}^{\text{GW}}). \quad (19)$$

The 1σ error can be obtained by

$$\sigma_{\ln d_L}^2 = \left(\frac{z_{i+1} - z}{z_{i+1} - z_i}\right)^2 \epsilon_{\ln d_{L,i}^{\text{GW}}}^2 + \left(\frac{z - z_i}{z_{i+1} - z_i}\right)^2 \epsilon_{\ln d_{L,i+1}^{\text{GW}}}^2,$$

where $\epsilon_{\ln d_{L,i}^{\text{GW}}} \equiv \epsilon_{d_{L,i}^{\text{GW}}}/d_{L,i}^{\text{GW}}$ is the distance uncertainty of the i th GW event (the mock GW catalogue has been sorted by redshift before interpolation).

3.1. The $E_{\text{iso}}-E_p$ correlation

We parameterize the Amati relation ($E_{\text{iso}}-E_p$ correlation) (Amati et al. 2002) as

$$\log_{10} \frac{E_{\gamma,\text{iso}}}{1 \text{ erg}} = a + b \log_{10} \left[\frac{E_{p,\text{obs}}(1+z)}{300 \text{ keV}} \right], \quad (20)$$

where $E_{p,\text{obs}}(1+z)$ is the cosmological rest-frame spectral peak energy of GRB. The Markov chain Monte Carlo (MCMC) algorithm is applied to constrain intercept a , slope b and intrinsic scatter σ_{int} of the correlation. We use the python module emcee to carry out parameters fitting (Foreman-Mackey et al. 2013). The likelihood to fit the linear relation $y = ax + b$ (D'Agostini 2005) is

$$L = \prod_{i=1}^N \frac{1}{\sqrt{2\pi} \sqrt{\sigma_{\text{int}}^2 + \sigma_{y_i}^2 + b^2 \sigma_{x_i}^2}} \exp \left[\frac{-(y_i - a - bx_i)^2}{2(\sigma_{\text{int}}^2 + \sigma_{y_i}^2 + b^2 \sigma_{x_i}^2)} \right]. \quad (21)$$

where $x \equiv \log_{10} \left[\frac{E_{p,\text{obs}}(1+z)}{300 \text{ keV}} \right]$, $y \equiv \log_{10} \frac{E_{\gamma,\text{iso}}}{1 \text{ erg}}$ and the propagated uncertainties of y is calculated from

$$\sigma_y^2 = \frac{\sigma_{S_{\text{bolo}}}^2}{(\ln 10 S_{\text{bolo}})^2}. \quad (22)$$

3.2. The $E_{\gamma}-E_p$ correlation

The parametrization of the Ghirlanda relation ($E_{\gamma}-E_p$ correlation) (Ghirlanda, Ghisellini & Lazzati 2004) is

$$\log_{10} \frac{E_{\gamma}}{1 \text{ erg}} = a + b \log_{10} \left[\frac{E_{p,\text{obs}}(1+z)}{300 \text{ keV}} \right]. \quad (23)$$

The likelihood function has the same form as $E_{\text{iso}}-E_p$ correlation's, while the propagated uncertainties of $y \equiv \log_{10} \frac{E_{\gamma}}{1 \text{ erg}}$ is calculated from

$$\sigma_y^2 = \frac{\sigma_{S_{\text{bolo}}}^2 F_{\text{beam}}^2 + (S_{\text{bolo}})^2 \sigma_{F_{\text{beam}}}^2}{(\ln 10 S_{\text{bolo}} F_{\text{beam}})^2}. \quad (24)$$

The same procedure as handling $E_{\text{iso}}-E_p$ correlation is used to calibrate the $E_{\text{iso}}-E_p$ correlation.

3.3. Results

With our mock GW catalogue, the constraints on intercept a and slope b of Amati relation is $a = 52.93 \pm 0.04$, $b = 1.41 \pm 0.07$, $\sigma_{\text{int}} = 0.39 \pm 0.03$ (1σ), while for Ghirlanda relation, $a = 50.63 \pm 0.08$, $b = 1.50 \pm 0.12$ and $\sigma_{\text{int}} = 0.16 \pm 0.04$ (1σ). The 1σ , 2σ and 3σ confidence contours and marginalized likelihood distributions are shown in Figure 2 and Figure 3 respectively. Wang & Wang (2016) standardized Amati relation of form $\log_{10}(E_{\gamma,\text{iso}}/\text{erg}) = a + b \log_{10}[E_{p,\text{obs}}(1+z)/\text{keV}]$ with SNe Ia Union2.1 sample. Their fitting results are $a = 48.46 \pm 0.033$, $b = 1.766 \pm 0.007$ with $\sigma_{\text{ext}} = 0.34 \pm 0.04$. Amati et al. (2018) calibrated Amati relation of form $\log_{10}(E_p/\text{keV}) = q + m[\log_{10}(E_{\text{iso}}^{\text{cal}}/\text{erg}) - 52]$, finding $q = 2.06 \pm 0.03$, $m = 0.50 \pm 0.12$ and $\sigma_{\text{int}} = 0.20 \pm 0.01$.

The calibrated GRB Hubble diagram is shown in Figure 4. The solid line in this figure is plotted based on the Planck15 cosmological parameters (Planck collaboration 2016).

3.4. Constraining Λ CDM model and cosmological applications

We combine the calibrated GRB data and SNe Ia from Pantheon sample (Scolnic et al. 2018) to constrain non-flat Λ CDM model. The nuisance parameters $\{\alpha, \beta, M_B^1, \Delta_M\}$ of SNe Ia lightcurve are fitted with cosmological parameters $\{\Omega_m, \Omega_\Lambda\}$ simultaneously with the following total likelihood function

$$L \propto L_{\text{GRB}} \cdot L_{\text{SN}},$$

The likelihood function of GRB is given by

$$L_{\text{GRB}} = \prod_{i=1}^N \frac{1}{\sqrt{2\pi} \sigma_{\mu_{\text{GRB},i}}} \exp \left[\frac{-(\mu_{\text{th},i} - \mu_{\text{GRB},i})^2}{2\sigma_{\mu_{\text{GRB},i}}^2} \right]. \quad (25)$$

where the distance modulus uncertainty $\sigma_{\mu_{\text{GRB}}}$ is

$$\sigma_{\mu_{\text{GRB}}}^2 = \left(\frac{5}{2} \sigma_{\log_{10} E_{\gamma, \text{iso}}} \right)^2 + \left(\frac{5}{2 \ln 10} \frac{\sigma_{S_{\text{bolo}}}}{S_{\text{bolo}}} \right)^2 \quad (26)$$

and

$$\sigma_{\log_{10} E_{\gamma, \text{iso}}}^2 = \sigma_a^2 + \left(\sigma_b \log_{10} \frac{E_{\text{p,obs}}(1+z)}{300 \text{ keV}} \right)^2 + \left(\frac{b}{\ln 10} \frac{\sigma_{E_{\text{p,obs}}}}{E_{\text{p,obs}}} \right)^2 + \sigma_{\text{int}}^2 \quad (27)$$

The Hubble constant H_0 in our fitting is fixed to Planck15 (Planck collaboration 2016) value. With the combined sample (GRBs + SNe), the best-fit values for non-flat Λ CDM model are $\Omega_m = 0.33 \pm 0.04$ and $\Omega_\Lambda = 0.52 \pm 0.08$ with 1σ uncertainties. The constraints on Ω_m , Ω_Λ and SNe Ia lightcurve parameters $\{\alpha, \beta, M_B^1, \Delta_M\}$ are shown in Figure 5.

4. SUMMARY

In this paper, we propose to calibrate the GRB luminosity relations using GW standard sirens. This method is model-independent and will overcome the circularity problem. The constraints for intercepts and slopes of Amati relation and Ghirlanda relation are $a = 52.93 \pm 0.04$, $b = 1.41 \pm 0.07$, $\sigma_{\text{int}} = 0.39 \pm 0.03$ (1σ) and $a = 50.63 \pm 0.08$, $b = 1.50 \pm 0.12$, $\sigma_{\text{int}} = 0.16 \pm 0.04$ (1σ) respectively with our mock GW catalogue. The performance of our method will improve with the upgrade of GW detector's sensitivity, especially with third generation detectors ET (Abernathy et al. 2011), BBO (Cutler & Holz 2009) and DECIGO (Kawamura et al. 2011). GRBs serve as a complementary tool to other cosmological probes such as SNe Ia, BAO and CMB. Besides, it plays a crucial role in constraining $w(z)$ especially at high redshifts (Wang, Qi & Dai 2011), which may help us understanding the nature of dark energy.

We thank the anonymous referee for constructive comments. We thank Wen Zhao, Tao Yang and Jun-Jie Wei for helpful suggestions. This work is supported by the National Natural Science Foundation of China (grant U1831207).

REFERENCES

- Ade, P. A. R., et al. (Planck collaboration), 2016, *A&A*, 594, A13
- Abadie, J., et al. (LIGO Scientific Collaboration), 2010, *Nucl. Instrum. Methods Phys. Res., Sect. A*, 624, 223 (2010)
- Abbott, B. P., et al. (LIGO Scientific Collaboration and Virgo Collaboration), 2017, *PhRvL*, 119, 161101
- Abernathy, M., et al., 2011, Einstein gravitational wave telescope: conceptual design study, European Gravitational Observatory, Document No. ET-0106C-10
- Amati, L., et al., 2002, *A&A*390, 81.
- Amati, L. 2006, *MNRAS*, 372, 233245
- Amati, L., et al. arXiv:1811.08934v1
- Arun, K. G., Iyer, B. R., Sathyaprakash, B. S., & Sundararajan, P. A. 2005, *PhRvD*, 71, 084008
- Avgoustidis, A., Verdec, L., & Jimenez, R. 2009, *JCAP*, 06, 012
- Band, D., et al. 1993, *ApJ*, 413, 281
- Barkana, R., & Loeb, A. 2004, *ApJ*, 601, 64
- Berger, E. 2007, *ApJ*, 670, 1254
- Blanchet, L., Faye, G., Iyer, B. R., & Joguet, B. 2002, *PhRvD*, 65, 061501
- Bloom, J. S., Frail, D. A., & Sari, R. 2001, *AJ*, 121, 2879
- Bromm, V., Coppi, P. S., & Larson, R. B. 2002. *ApJ*, 564, 23
- Cai, R. G., & Yang, T. 2017, *PhRvD*, 95, 044024
- Cucchiara, A., et al. 2011, *ApJ*, 736, 7
- Cutler, C., & Holz, D. E. 2009, *PhRvD*, 80, 104009
- G. DAgostini, G. 2005, arXiv:physics/0511182v1
- Dai, Z. G., Liang, E. W., & Xu, D. 2004, *ApJ*, 612, L101
- Dainotti, M.G., Cardone, V.F., Capozziello, S., 2008, *MNRAS*, 391, L79
- Dainotti, M. G., & Del Vecchio, R. 2017, *New Astronomy Reviews*, 77, 23
- Dainotti, M. G., Ostrowski, M., & Willingale, R. 2011, *MNRAS*, 418, 2202
- Dainotti, M. G., Del Vecchio, R., & Tarnopolski, . 2018, *Advances in Astronomy*, 4969503
- Dainotti, M. G., & Amati, L. 2018, *PASP*, 130, 051001
- Foreman-Mackey, D., et al. 2013, *PASP*, 125, 306
- Fryer, C. L., & Kalogera, V. 2001, *ApJ*, 554, 548
- Ghirlanda, G., Ghisellini, G., & Lazzati, D. 2004, *ApJ*, 616, 331
- Ghirlanda, G., et al. 2004, *ApJ*, 613, L13
- Ghirlanda, G., et al. 2006, *A&A*, 452, 839
- Ghisellini, G., et al. 2009, *MNRAS*, 393, 253
- Hartoog, O. E. et al., 2015, *A&A*, 580, A139
- Holz, D. E. 1998, *ApJ*, 506, L1
- Hu, J., Yu, H., & Wang, F. Y. 2017, *ApJ*, 836, 107
- Hui, L., & Greene, P. B. 2006, *PhRvD*, 73, 123526
- Kawamura, S., et al. 2011, *Class. Quantum Grav.* 28, 094011
- Kodama, Y., et al. 2008, *MNRAS*, 391, L1.
- Kumar, P., & Zhang, B. 2015, *PhR*, 561, 1

- Li, H., et al. 2008, ApJ, 680, 92
- Li, T. G. F., *Extracting Physics from Gravitational Waves* (Springer Theses, New York, 2015)
- Liang, E. W., & Zhang, B. 2005, ApJ, 633, 611
- Liang, E.W., & Zhang, B. 2006. MNRAS, 369, L37
- Liang, E. W., Zhang, B. B., & Zhang, B. 2007, ApJ, 670, 565
- Liang, N., Xiao, W. K., Liu, Y., & Zhang, S. N. 2008, ApJ, 685, 354
- Liang, E. W., et al. 2015, ApJ, 813, 116
- Norris, J. P., Marani, G. F., Bonnell, J. T. 2000, ApJ, 534, 248
- Oates, S. R., et al. 2012, MNRAS, 426, L86
- Rodney, S. A., et al. 2015, AJ, 150, 156
- Sathyaprakash, B. S., B F Schutz, B. F., & Van Den Broeck, C. 2010, *Class. Quantum Grav.* 27, 215006
- Schaefer, B. E. 2007, ApJ, 660, 16
- Schneider, R., et al. 2001, MNRAS, 324, 797
- Schutz, B. F. 1986, *Nature (London)* 323, 310
- Scolnic, D. M., et al. 2018, ApJ, 859, 101
- Totani, T. 1997, ApJ, 486, L71
- Totani, T., et al. 2006, PASJ, 58, 485
- Wang, F. Y., Dai, Z. G., & Zhu, Z. H. 2007, ApJ, 667, 1
- Wang, F. Y., & Dai, Z. G. 2009, MNRAS, 400, L10
- Wang, F. Y., & Dai, Z. G. 2011, A&A, 536, A96
- Wang, F. Y., et al. 2012, ApJ, 760, 27
- Wang, F. Y. 2013, A&A, 556, A90
- Wang, F. Y., Dai, Z. G., & Liang, E. W. 2015, *New Astronomy Reviews*, 67, 1
- Wang, F. Y., Qi, S., & Dai, Z. G. 2011, MNRAS, 415, 3423
- Wang, J. S., Wang, F. Y., Cheng, K. S., & Dai, Z. G. 2016, A&A, 585, A68
- Wang, Y. 2008, PhRvD, 78, 123532
- Wei, D. M., & Gao, W. H. 2003, MNRAS, 345, 743
- Yonetoku, D., et al. 2004, ApJ, 609, 935
- Zhao, W., Van Den Broeck, C., Baskaran, D., & Li, T. G. F. 2011, PhRvD, 83, 023005
- Zhao, W., & Wen, L. Q. 2018, PhRvD, 97, 064031

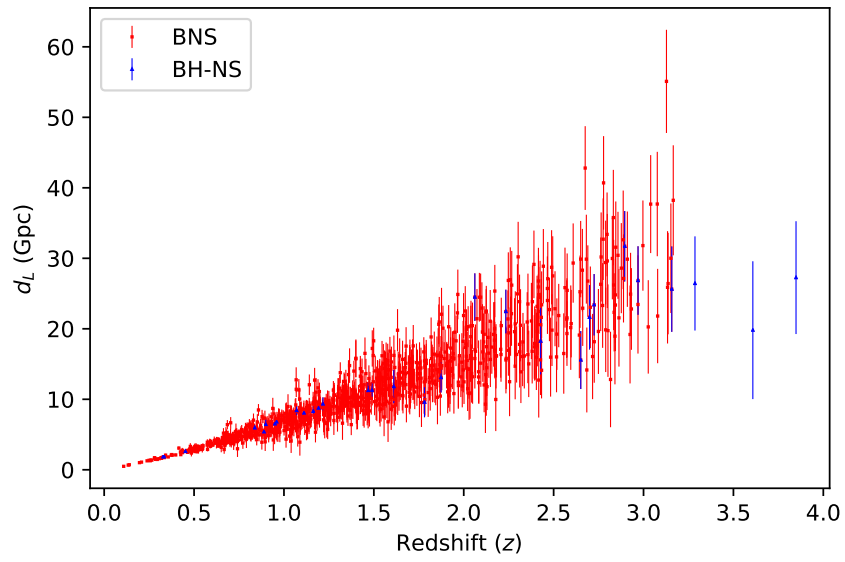


Figure 1. Mock GW catalogue of 1000 BNS merger events and 30 BH-NS merger events as standard sirens.

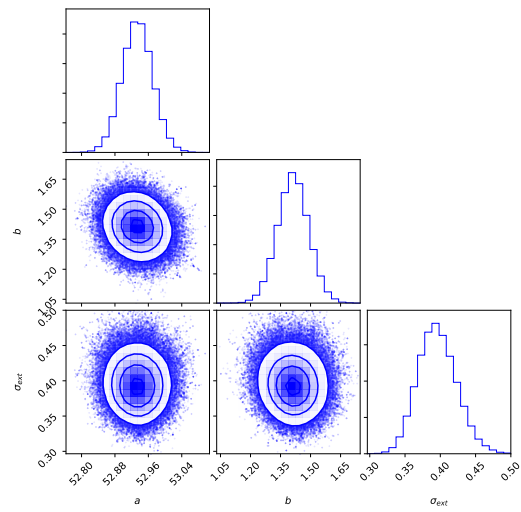


Figure 2. Confidence contours (1σ , 2σ and 3σ) and marginalized likelihood distributions for intercept a and slope b in Amati relation.

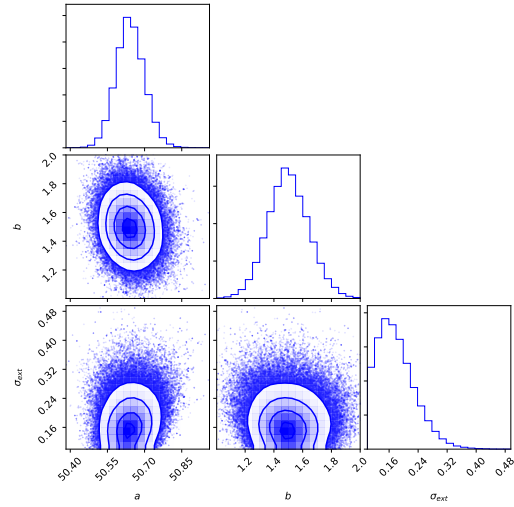


Figure 3. Confidence contours (1σ , 2σ and 3σ) and marginalized likelihood distributions for intercept a and slope b in Ghirlanda relation.

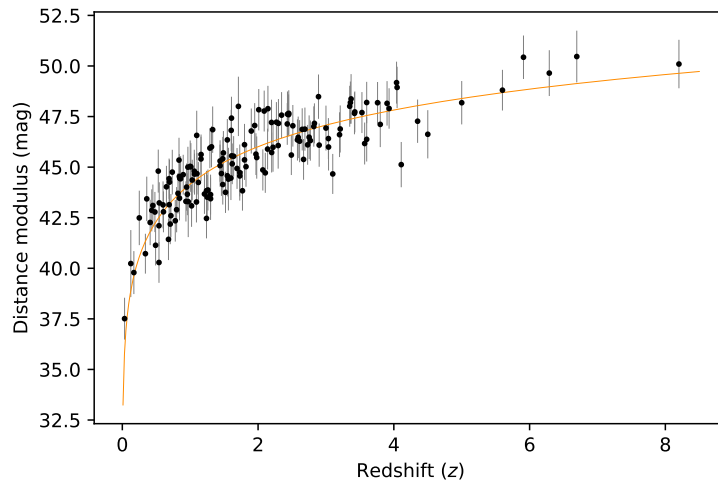


Figure 4. Distance modulus of calibrated GRBs in comparison to Planck15 (Planck collaboration 2016) Λ CDM cosmology (depicted in solid orange line).

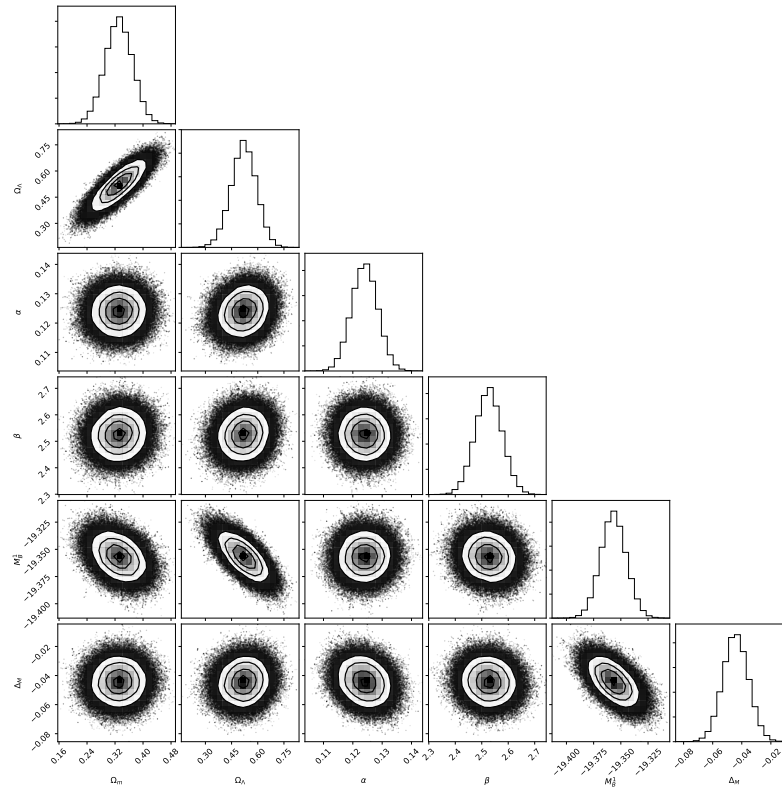


Figure 5. 1σ , 2σ and 3σ constraints on Ω_m , Ω_Λ and SNe Ia lightcurve parameters $\{\alpha, \beta, M_B^1, \Delta_M\}$ from "calibrated" GRB and Pantheon SNe Ia sample.